mRNA decapping machinery targets *LBD3/ASL9* transcripts to allow developmental changes in *Arabidopsis*

Zhangli Zuo[1], Milena Edna Roux[2], Jonathan Renaud Chevalier[1], Yasin F. Dagdas[3], Takafumi Yamashino[4], Søren Diers Højgaard[1], Emilie Knight[5], Lars Østergaard[5], Eleazar Rodriguez[1] & Morten Petersen[1,*]

[1] Department of Biology, Faculty of Science, University of Copenhagen, Copenhagen, Denmark
[2] Novo Nordisk, Regulatory Affairs Durable Devices and Needles, Søborg, Denmark
[3] Gregor Mendel Institute, Austrian Academy of Sciences, Vienna BioCenter, Vienna, Austria
[4] Laboratory of Molecular Microbiology, School of Agriculture, Nagoya University, Nagoya, Japan
[5] Crop Genetics Department, John Innes Centre, Norwich Research Park, Norwich NR4 7UH, United Kingdom

*Corresponding author. Tel: +45 35322127; E-mail: shutko@bio.ku.dk

Abstract

Multicellular organisms perceive and transduce multiple cues to optimize development and cell state switching. Key transcription factors drive developmental changes, but transitions also require the attenuation of previous states and removal of negative regulators. Here, we report shared developmental defects in apical hook, primary and lateral root growth in multiple decapping deficient mutants. The mRNA levels of *LATERAL ORGAN BOUNDARIES DOMAIN 3 (LBD3)/ASYMMETRIC LEAVES 2-LIKE 9 (ASL9)* transcription factor are directly regulated by mRNA decapping machinery. More specifically, *ASL9* transcripts accumulate in decapping deficient plants and can be found in complexes with decapping components. Accumulation of *ASL9* inhibits apical hook, primary root growth and lateral root formation. Interestingly, exogenous auxin application restores lateral roots formation in both *ASL9* over-expressors and mRNA decay-deficient mutants. Moreover, mutations in the cytokinin transcription factors type-B ARABIDOPSIS RESPONSE REGULATORS (B-ARRs) *ARR10* and *ARR12* restore the developmental defects caused by over-accumulation of capped *ASL9* transcript upon *ASL9* overexpression. Most importantly, loss-of-function of *asl9* partially restores apical hook, primary root growth and lateral root formation in decapping deficient mutants. Thus, the mRNA decay machinery directly targets *ASL9* transcripts for decay to balance cytokinin/auxin responses during development.

Introduction

Understanding normal tissue development requires information about diverse cellular mechanisms controlling gene expression. Much work has focused on of the transcriptional networks that govern stem cell differentiation. For example, ectopic expression of Yamanaka factors may lead to induced pluripotency in mice and humans (Takahashi and Yamanaka, 2006; Yu et al., 2007). Similarly, ectopic expression of *LATERAL ORGAN BOUNDARIES DOMAIN (LBD)/ASYMMETRIC LEAVES2-LIKE (ASL)* genes is sufficient to induce spontaneous proliferation of pluripotent cell masses in plants, a reprogramming process triggered *in vitro* by complementary/Yin-Yang phytohormones auxin and cytokinin (Fan et al., 2012; Schaller et al., 2015). Auxin and cytokinin responses are essential for a vast number of developmental processes in plants including post-embryonic reprograming and formation of the apical hook to protect the meristem during germination in darkness (Chaudhury et al., 1993; Hu et al., 2017) as well as lateral root (LR) formation (Jing and Strader, 2019). Loss-of-function mutants in

genes that regulate auxin-dependent transcription such as *auxin-resistant1* exhibit defective hooking and LR formation (Estelle and Somerville, 1987; Lehman et al., 1996). In addition, type-B ARABIDOPSIS RESPONSE REGULATORS (B-ARRs) ARR1, ARR10 and ARR12 work redundantly to activate cytokinin transcriptional responses which regulated by negative feedback type-A ARRs in shoot development and LR formation (Riefler et al., 2006; Ishida et al., 2008; Xie et al., 2018). Exogenous cytokinin application disrupts LR initiation by blocking pericycle founder cell transition from G2 to M phase (Li et al., 2006). Thus, reshaping the levels of certain transcription factors leads to changes in cellular identity. As developmental programming must be tightly regulated to prevent spurious development, the expression of these transcription factors may be controlled at multiple levels (Tatapudy et al., 2017). However, most developmental studies focus on their transcription rates and overlook the contribution of mRNA stability or decay to these events (Crisp et al., 2016).

Eukaryotic mRNAs contain stability determinants including the 5' 7-methylguanosine triphosphate cap (m7G) and the 3' poly-(A) tail. mRNA decay is initiated by deadenylation, followed by degradation via either 3'-5' exosomal exonucleases and SUPPRESSOR OF VCS (SOV)/DIS3L2 or via the 5'-3' exoribonuclease activity of the decapping complex (Garneau et al., 2007; Sorenson et al., 2018). This complex includes the decapping holoenzyme composed of the catalytic subunit DCP2 and its cofactor DCP1 along with other factors (DCP5, DHH1, VCS, LSM1-7 complex and PAT1), and the exoribonuclease XRN that degrades monophosphorylated mRNA. As a central platform, PAT1 (Protein Associated with Topoisomerase II, PAT1b in mammals) forms a heterooctameric complex with LSM(Like-sm)1-7 at 3' end of a mRNA to engage transcripts containing deadenylated tails thereafter recruits other decapping factors and interacts with them using different regions, these decapping complex and mRNAs can aggregate into distinct cytoplasmic foci called processing bodies (PBs) (Brengues et al., 2005; Balagopal and Parker, 2009;Ozgur et al., 2010; Chowdhury et al., 2014; Charenton et al., 2017; Lobel et al., 2019). Beyond *DCP* genes, deletion of *PAT1* gene in yeast exhibits the strongest temperature sensitive phenotype compared to other decapping factors genes (Bonnerot et al., 2000).

mRNA decay regulates mRNA levels and thereby impacts cellular state switching (Newman et al., 2017; Essig et al., 2018). We and others have shown that the decapping machinery is involved in stress and immune responses (Xu and Chua, 2012; Merret et al., 2013; Roux et al., 2015; Perea-Resa et al., 2016; Crisp et al., 2017; Yu et al., 2019), and that RNA binding proteins can target selected mRNAs for decay

(Gerstberger et al., 2014; Perea-Resa et al., 2016; Yu et al., 2019). Postembryonic lethality (Xu et al., 2006) and stunted growth phenotypes (Xu and Chua, 2009; Perea-Resa et al., 2012) associated with disturbance of the decay machinery indicate the importance of mRNA decapping and decay machinery during plant development. However, while much has been learned about how mRNA decapping regulates plant stress responses (Perea-Resa et al., 2016; Yu et al., 2019; Zuo et al., 2021), far less is known about how decapping contributes to plant development.

Arabidopsis dcp1, *dcp2* and *vcs* mutants display postembryonic lethality whereas *lsm1alsm1b* and *dcp5* knock-down mutants only exhibit abnormal development. *Arabidopsis* encodes two *LSM1* genes and three *PAT* paralogs and *lsm1alsm1b* double and *pat* triple mutants are dwarfs and *dcp5* displays a delayed growth phenotype (Xu et al., 2006; Xu and Chua, 2009; Perea-Resa et al., 2012; Zuo et al., 2022a; Zuo et al., 2022b). All these differences suggest that mutations in mRNA decay components may cause pleiotropic phenotypes not directly linked to mRNA decapping and decay deficiencies (Riehs-Kearnan et al., 2012; Gloggnitzer et al., 2014; Roux et al., 2015). For example, it has been proposed that lethality in some mRNA decay loss-of-function mutants is not due to decay deficiencies *per se*, but to the activation of immune receptors which evolved to surveil microbial manipulation of the decay machinery (Roux et al., 2015). In line with this, loss-of-function of *AtPAT1* inappropriately triggers the immune receptor SUMM2, and *Atpat1* mutants consequently exhibit dwarfism and autoimmunity (Roux et al., 2015). Thus, PAT1 is under immune surveillance and PAT proteins are best studied in SUMM2 loss-of-function backgrounds.

Here we study the impact of perturbed mRNA decapping during development. For this, we have analyzed 3 sequential mRNA decapping mutants *dcp2-1*, *dcp5-1* and *pat* triple mutant (*pat1-1path1-4path2-1summ2-8*) mRNA decay-deficient mutants, revealing that the mRNA decay machinery directly regulates the important developmental regulator *ASL9*. Thus, when mRNA decay is disrupted, *ASL9* accumulates and contributes to inhibit cells from forming apical hooks and lateral roots. Moreover, interference with a cytokinin pathway and/or exogenous auxin application restores the developmental defects in both *ASL9* over-expressing plants and in mRNA decay deficient mutants. Markedly, mutation in *asl9* also partially restores the developmental defects including apical hook and lateral root formation and primary root elongation in decapping mutants. These observations indicate that the mRNA decay machinery is fundamental to developmental decision making.

Results

mRNA decapping deficiency causes deregulation of apical hooking

We and others have reported that mutants of mRNA decay components exhibit abnormal developmental phenotypes including postembryonic death and stunned growth (Xu et al., 2006; Xu and Chua, 2009; Perea-Resa et al., 2012; Roux et al., 2015; Zuo et al., 2022b), indicating mRNA decay may be needed for proper development. To assess this, we explored readily scorable phenotypic evidence of defective decision-making during development. Since apical hooking can be exaggeratedly induced by exogenous application of ethylene or its precursor ACC, we germinated seedlings in darkness in the presence or absence of ACC (Bleecker et al., 1988; Guzman and Ecker, 1990). Interestingly, all the mRNA decapping mutants tested, *dcp2-1*, *dcp5-1* and *pat* triple mutant were hookless and unable to make the exaggerated apical hook under ACC treatment (Fig. 1A, B, S1A&B) being that *dcp2-1* exhibit the strongest hookless phenotype. Since *dcp2-1* is postembryonic lethal, we used seeds from a parental heterozygote to score for hook formation, and subsequentially confirmed by genotyping that all hookless seedlings were *dcp2-1* homozygotes. This indicates that mRNA decapping is required for the commitment to apical hooking. Supporting this notion, ACC treatment led to a massive increase of DCP5-GFP (Chicois et al., 2018) and Venus-PAT1(Zuo et al., 2022b) foci in hook regions (Fig.1C). Collectively, these data show that mRNA decay may be involved in apical hook formation.

mRNA decay machinery targets *ASL9* for decay

To search for transcripts responsible for the hookless phenotype, we revisited our previous RNA-seq data for *pat* triple mutant (Zuo et al., 2022b) and verified that transcripts of *ASL9* (*ASYMMETRIC LEAVES 2-LIKE 9*, also named *LBD3, LOB DOMAIN-CONTAINING PROTEIN 3*) accumulated specifically in *pat* triple mutants (Zuo et al., 2022b). ASL9 belongs to the large AS2/LOB (ASYMMETRIC LEAVES 2/LATERAL ORGAN BOUNDARIES) family (Matsumura et al., 2009) which includes key regulators of organ development (Xu et al., 2016). Interestingly, the ASL9 homologue ASL4 negatively regulates brassinosteroids accumulation to limit growth in organ boundaries, and overexpression of *ASL4* impairs apical hook formation and leads to dwarfed growth (Bell et al., 2012). While *ASL4* mRNA did not accumulate in *pat* triple mutants (Data Set S1), we hypothesized that ASL9 could also interfere with

apical hook formation. We therefore analyzed mRNA levels of *ASL9* in ACC-treated seedlings and verified that all 3 mRNA decapping mutants *dcp2-1, dcp5-1* and *pat* triple mutants accumulated up to 30-fold higher levels of *ASL9* transcript compared to ACC treated Col-0 seedlings (Fig. 2A). Concordantly, two over-expressor lines of *ASL9* Col-0/*oxASL9* and Col-0/*oxASL9-VP16* (Naito et al., 2007) also exhibited hookless phenotypes (Fig. 2B&C). However, we did not observe any changes including tighter apical hooks in *asl9-1* mutants (Fig. S1C&D) suggesting other members of the AS2/LOB family act redundantly in this process. Nevertheless, these results indicate that apical hook formation in mRNA decapping deficient mutants is compromised, in part, due to misregulation of *ASL9*.

To determine whether *ASL9* is a target of the decapping complex, we performed 5'-RACE assays and found more capped *ASL9* in mRNA decapping mutant seedlings compared to Col-0 (Fig 2D). We also assayed for capped *ASL9* transcripts in ACC and mock-treated mRNA decapping mutants. By calculating the ratio between capped versus total *ASL9* transcripts, we verified that with ACC treatment, mRNA decapping mutants accumulated significantly higher levels of capped *ASL9* transcripts than Col-0 (Fig. 2E). Moreover, RNA immunoprecipitation (RIP) revealed enrichment of *ASL9* in DCP5-GFP and Venus-PAT1 plants compared to a free YFP control line (YFP-WAVE) (Fig. 2F), indicating mRNA decapping components directly bind *ASL9* transcripts. These data confirms that *ASL9* mRNA can be found in mRNA decapping complexes, and that mRNA decapping contributes to ACC-induced apical hook formation by regulating *ASL9* mRNA levels.

Accumulation of *ASL9* suppresses LR formation and primary root growth

LR formation is another example of post embryonic decision making. In *Arabidopsis* the first stage of LR formation requires that xylem pericyle pole cells change fate to become LR founder cells, a process positively regulated by auxin and negatively regulated by cytokinin and ethylene (Jung and McCouch, 2013; Weijers et al., 2018). As *ASL9* has been implicated in cytokinin signaling (Naito et al., 2007) and the cytokinin signaling repressors type-A ARR genes *ARR3, ARR4, ARR8* and *ARR15* and the auxin efflux gene *PIN5*, auxin induced gene *SAUR23* and *IAA19* and auxin biosynthesis gene *TAR2* are repressed in both *pat* triple mutant and Col-0/*oxASL9* (Fig. S2), we therefore examined LR formation in *dcp5-1* and *pat* triple mutants and in both *ASL9* over-expressors. LR formation was almost absent in *dcp5-1*, *pat* triple mutants, Col-0/*oxASL9* and Col-0/*oxASL9-VP16* (Fig. 3A, B, S3A&B). However, like

seen for apical hooking, *asl9-1* also appeared to display normal LR formation (Fig. S3C&D). Nevertheless, LR formation defects in *dcp5-1* and *pat* triple mutants indicates that mRNA decapping is required for the commitment to LR formation, a process positively regulated by auxin. Supporting this notion, auxin treatment led to a massive increase of DCP5-GFP and Venus-PAT1 foci in root regions. As primary root development is also regulated by auxin signaling (Billou et al., 2005; Brumos et al., 2018), we examined primary root growth in mRNA decapping mutants and *ASL9* over-expressor. Again *dcp5-1*, *pat* triple mutants, Col-0/*oxASL9* and Col-0/*oxASL9-VP16* exhibit reduced primary root length (Fig 3A&B). Collectively, these data indicate mRNA decapping machinery, targeting *ASL9*, contributes to LR formation and primary root extension.

Interference of a cytokinin pathway and/or exogenous auxin restores developmental defects of *ASL9* over-expressor and mRNA decay deficient mutants

ASL9 has been implicated in cytokinin signaling (Naito et al., 2007) in which ARR1, ARR10 and ARR12 are responsible for activation of cytokinin transcriptional responses (Ishida et al., 2008; Xie et al., 2018) and cytokinin acts antagonistically with auxin. Apical hooking and lateral root formation are classic examples of auxin dependent developmental reprogramming (Peer et al., 2011). Since cytokinin signaling repressor genes and auxin responsive genes are repressed in both mRNA decay mutants and in Col-0/*oxASL9*, we hypothesized that the developmental defects of mRNA decay mutants and Col-0/*oxASL9* are due to repressed auxin responses possibly caused by persistent cytokinin signaling (Fig S3). To test this, we examined the developmental phenotype of *ASL9* over-expressors in *arr10-5arr12-1* mutants (Ishida et al., 2008). Interestingly, all apical hooking, LR formation and primary root elongation phenotypes of *ASL9* over-expressors were largely restored in this background (Fig. 4). To study this in more detail, we introduced the indirect auxin-responsive reporter *DR5*::GFP in Col-0, *dcp5-1* and *dcp2-1*. We found increased GFP signals in the concave side of Col-0 hook region but not in *dcp5-1* or *dcp2-1* and the overall GFP signals in *dcp2-1* were markedly lower than Col-0 (Fig. S4). We also examined DR5-GFP signal in root area of 7-day old Col-0 and *dcp5-1* seedlings, again, overall GFP signal in *dcp5-1* were strikingly lower than Col-0 (Fig S5). Collectively these data indicate repressed auxin responses during apical hook and root developmental processes in the decapping mutants. We then applied exogenous auxin to mRNA decay mutants *dcp5-1* and *pat* triple and Col-0/*oxASL9*. This showed that 0.2 µM IAA could partially restore LR formation in *dcp5-1*, *pat* triple and Col-0/*oxASL9* (Fig. S6).

These findings indicate that the mRNA decay machinery targets *ASL9* to help keep cytokinin/auxin responses balanced during development.

ASL9 directly contributes to apical hooking, LR formation and primary root growth

The overexpression of *ASL9* is sufficient to suppress apical hook and lateral root development and primary root growth. To examine if *ASL9* accumulation directly contributes to the developmental defects in decapping mutants, we crossed *asl9-1* and *dcp5-1* to generate *dcp5-1/asl9-1* double mutants. We then germinated *dcp5-1/asl9-1* seedlings in darkness in the presence or absence of ACC and in both conditions *dcp5-1/asl9-1* made more stringent hooks than *dcp5-1* but not as tight as Col-0 or *asl9*-1 did, indicating that the loss-of-function of *asl9* can partially suppress *dcp5-1* hookless phenotype (Fig. 5A &B). Moreover, the LR and primary root phenotype of *dcp5-1* was also partially restored by mutating *ASL9* (Fig 5C-E). Overall, our data indicates that *ASL9* directly contributes to apical hooking, LR development and primary root growth.

Discussion

Cellular state switching requires massive overhauls of gene expression (Miyamoto et al., 2015). Apart from unlocking effectors needed to install a new program, previous states or programs also need to be terminated (Tatapudy et al., 2017; Rodriguez et al., 2020). We report here that mRNA decay is required for certain auxin dependent developmental processes. The stunted growth phenotype and downregulation of developmental and auxin responsive mRNAs in the mRNA decapping mutant (Zuo et al., 2022b) supports a model in which defective clearance of mRNAs hampers decision making upon hormonal perception. Apical hooking and LR formation are classic examples of auxin-dependent developmental processes (Peer et al., 2011). In line with this, we and others observed that mRNA decay-deficient mutants are impaired in apical hooking (Fig. 1) and LR formation (Fig. 3) (Perea-Resa et al., 2012; Jang et al., 2019). Interestingly, among the transcripts upregulated in these decay-deficient mutants was that of capped *ASL9/LBD3* (Fig. 2), which is involved in cytokinin signaling (Naito et al., 2007). Cytokinin and auxin can act antagonistically (Su et al., 2011), and cytokinin can both attenuate apical hooking (Tantikanjana et al., 2001) and directly affect LR founder cells to prevent initiation of lateral root primordia (Laplaze et al., 2007). Our findings that defective processing during those developmental

events in mRNA decay-deficient mutants involves *ASL9* was supported by our observation that *ASL9* mRNA is directly regulated by the decapping machinery and that Col-0/*oxASL9* transgenic lines cannot reprogram to attain an apical hook or to form LRs (Fig. 2&3) while loss-of-function of *asl9* partially restores the developmental defects in the decapping deficient mutants (Fig. 5). In line with this, we speculate that the inability to terminate cytokinin-dependent programs prevents the correct execution of auxin-dependent reprograming in mRNA decay-deficient mutants. This is supported by the observation that auxin responses in the *dcp5-1* and *dcp2-1* mutants are repressed (Fig. S4&5) and treating *dcp5-1, pat* triple and Col-0/*oxASL9* with exogenous auxin partially restores LR formation (Fig. S6). In line with this, the defects in both apical hooking and LR formation of *ASL9* over-expressing plants are largely restored by knocking out 2 cytokinin signaling activator genes *ARR10* and *ARR12* (Fig. 4).

Arabidopsis contains 42 *LBD/ASL* genes (Matsumura et al., 2009), among these genes *LBD16*, *LBD17*, *LBD18* and *LBD29* control lateral roots formation and regulate plant regeneration (Fan et al., 2012) and overexpression of another member *ASL4* also impairs apical hook (Bell et al., 2012). The partial restoration of apical hooking and LR formation caused by *asl9* mutation in *dcp5-1* (Fig. 5) suggest that other *ASL*s and/or non-*ASL* genes may also contribute to the developmental defects in decapping mutants. Besides lateral root formation, it was recently reported that *Arabidopsis* LBD3, together with LBD4, functions as rate-limiting components in activating and promoting root secondary growth, which is also tightly regulated by auxin and cytokinin, indicating that LBDs balance primary and secondary root growth (Smetana et al., 2019; Xiao et al., 2020; Smith et al., 2020; Ye et al., 2021).

Deadenylated mRNA can be degraded via either 3'-5' exosomal exonucleases and SUPPRESSOR OF VCS (SOV)/DIS3L2 or via the 5'-3' exoribonuclease activity of the decapping complex (Garneau et al., 2007; Sorenson et al., 2018). Sorenson et al. (2018) found that *ASL9* expression is dependent on both VCS and SOV based on their transcriptome analysis, so that *ASL9* might be a substrate of both pathways (Sorenson et al., 2018). While more direct data is needed to conclude whether SOV can directly regulate *ASL9* mRNA levels, we have shown that *ASL9* is a target of the mRNA decapping machinery. However, since the Col-0 accession is a *sov* mutant and has no developmental defects, the SOV decay pathway probably only plays a minor role. The function of PBs in mRNA regulation has been controversial since mRNAs in PBs may be sequestered for degradation or re-enter polysomal translation complexes (Franks and Lykke-Andersen, 2008). Yeast PAT1 has also been found to repress translation (Coller and Parker,

2005) and a recent study has confirmed that PBs function as mRNA reservoirs in dark-grown *Arabidopsis* seedlings (Jang et al., 2019). These data open the possibility that *ASL9* might be also regulated at the protein level by the decapping machinery. Nevertheless, our finding of direct interaction of *ASL9* transcripts with DCP5 and PAT1, together with the accumulation of capped *ASL9* in mRNA decay mutants, indicates that *ASL9* misregulation in *dcp2-1*, *dcp5-1* and *pat* triple mutants is at least in part due to mRNA decapping deficiency (Fig. 2).

Materials and Methods

Plant materials and growth conditions

Arabidopsis thaliana ecotype Columbia (Col-0) was used as a control. All mutants used in this study are listed in Table S1. T-DNA insertion lines for AT5G13570(*DCP2*) *dcp2-1* (Salk_000519), At1g26110 (*DCP5*) *dcp5-1* (Salk_008881) and double mutant *arr10-5/arr12-1* has been described (Xu et al., 2006; Ishida et al., 2008; Xu and Chua, 2009). The T-DNA line for for AT1g16530 (*ASL9*) is SAIL_659_D08 with insertion in the first exon. Primers for newly described T-DNA lines are provided in Table S2. *pat* triple mutant, Venus-PAT1 and DCP5-GFP transgenic line have also been described (Zuo et al., 2022b; Chicois et al., 2018). The YFP WAVE line was from NASC (Nottingham, UK) (Geldner et al., 2009). Col-0/*oxASL9* line has been described before (Naito et al., 2007).

Plants were grown in 9×9cm or 4×5cm pots at 21°C with 8/16hrs light/dark regime, or on plates containing Murashige–Skoog (MS) salts medium (Duchefa), 1% sucrose and 1% agar with 16/8hr light/dark.

Plant treatments

For ethylene triple response assays, seeds were plated on normal MS and MS+50µM ACC, vernalized 96hrs and placed in the dark at 21°C for 4 days before pictures were taken. Apical hook angle is defined as 180° minus the angle between the tangential of the apical part with the axis of the lower part of the hypocotyl, in the case of hook exaggeration, 180° plus that angle is defined as the angle of hook curvature (Vandenbussche et al., 2010). Cotyledon and hook regions of etiolated seedlings were collected after placing in the dark at 21°C for 4 days for gene expression and XRN1 assay. For LR formation assays,

seeds on MS plates were vernalized 96hrs and grown with 16/8 hrs light/dark at 21°C vertically for 10 days. For external IAA application for LR formation experiments, seeds on MS plates were vernalized 96hrs and grown with 16/8 hrs light/dark at 21°C for 7 days and the seedlings were moved to MS or MS+IAA plates and grown vertically for 7 days.

Cloning and transgenic lines

pGreenIIM DR5V2-ntdtomato/DR5-n3GFP has been published previously (Liao et al., 2015). Arabidopsis transformation was done by floral dipping (Clough and Bent, 1998). *arr10-5arr12-1/oxASL9* was generated by vacuum infiltrating *arr10-5arr12-1* with *A. tumefaciens* strain EHA101 harbouring pSK1-ASL9(Naito et al., 2007). Transformants were selected on hygromycin (30 mg/L) or methotrexate (0.1mg/L) MS agar, and survivors tested for transcript expression by qRT-PCR and protein expression by immuno-blotting.

Protein extraction, SDS-PAGE and immunoblotting

Tissue was ground in liquid nitrogen and 4×SDS buffer (novex) was added and heated at 95°C for 5 min, cooled to room temperature for 10min, samples were centrifuged 5min at 13000 rpm. Supernatants were separated on 10% SDS-PAGE gels, electroblotted to PVDF membrane (GE Healthcare), blocked in 5% (w/v) milk in TBS-Tween 20 (0.1%, v/v) and incubated 1hr to overnight with primary antibodies (anti-GFP (AMS Biotechnology 1:5.000)). Membranes were washed 3 × 10 min in TBS-T (0.1%) before 1hr incubation in secondary antibodies (anti-rabbit HRP or AP conjugate (Promega; 1: 5.000)). Chemiluminescent substrate (ECL Plus, Pierce) was applied before camera detection. For AP-conjugated primary antibodies, membranes were incubated in NBT/BCIP (Roche) until bands were visible.

Confocal microscopy

Imaging was done using a Leica SP5 inverted microscope. The confocal images were analyzed with Zen2012 (Zeiss) and ImageJ software. Representative maximum intensity projection images of 10 Z-stacks per image have been shown in Fig. 1,3&S4.

RNA extraction and qRT-PCR

Total RNA from tissues was extracted with TRIzol™ Reagent (Thermo Scientific), 2µg total RNA were treated with DNAse I (Thermo Scientific) and reverse transcribed into cDNA using RevertAid First Strand cDNA Synthesis Kit according to the manufacturer's instructions (Thermo Scientific). The *ACT2* gene was used as an internal control. qPCR analysis was performed on a Bio-RAD CFX96 system with SYBR Green master mix (Thermo Scientific). Primers are listed in Table S2. All experiments were repeated at least three times each in technical triplicates.

In Vitro XRN1 Susceptibility Assay

Transcripts XRN1 susceptibility was determined as described (Mukherjee et al. 2012; Kiss et al., 2016) with some modification. Total RNA was extracted from tissues using the NucleoSpin® RNA Plant kit (Machery-Nagel). 1µg RNA was incubated with either 1 unit of XRN1 (New England Biolabs) or water for 2hr at 37°C, loss of ribosomal RNA bands on gel electrophoresis was used to ensure XRN1 efficiency, after heating inactivation under 70°C for 10min, half of the digest was then reverse transcribed into random primed cDNA with RevertAid First Strand cDNA Synthesis Kit (Thermo Scientific). Capped target transcript accumulation was measured by comparing transcript levels from XRN1-treated versus mock-treated samples using qPCR (EIF4A1 serves as inner control) for the individual genotypes (Mukherjee et al. 2012; Roux et al., 2015; Kiss et al., 2016).

RIP assay

RIP was performed as previously described (Streitner et al., 2012). 1.5g tissues were fixated by vacuum infiltration with 1% formaldehyde for 20min followed by 125 mM glycine for 5min. Tissues were ground in liquid nitrogen and RIP lysis buffer (50mM Tris-HCl pH 7.5; 150mM NaCl; 4mM MgCl2; 0.1% Igepal; 5 mM DTT; 100 U/mL Ribolock (Thermo Scientific); 1 mM PMSF; Protease Inhibitor cocktail (Roche)) was added at 1.5mL/g tissue powder. Following 15 min centrifugation at 4°C and 13000rpm, supernatants were incubated with GFP Trap-A beads (Chromotek) for 4 hours at 4°C. Beads were washed 3 times with buffer (50 mM Tris-HCl pH 7.5; 500 mM NaCl; 4 mM MgCl2; 0.5 % Igepal; 0.5 % Sodium deoxycholate; 0.1 % SDS; 2 M urea; 2 mM DTT before RNA extraction with TRIzol™ Reagent (Thermo Scientific)). Transcript levels in input and IP samples were quantified by qPCR, and levels in IP samples were corrected with their own input values and then normalized to YFP WAVE lines for enrichment.

5'-RACE assay

5'-RACE assay was performed using the First Choice RLM-RACE kit (Thermo Scientific) following manufacture's instruction. RNAs were extracted from 4-day-old etiolated seedlings with the NucleoSpin® RNA Plant kit (Machery-Nagel), and PCRs were performed using a low (26-28) or high (30-32) number of cycles. Specific primers for the 5' RACE adapter and for the genes tested are listed in Table S2.

Statistical analysis

Statistical details of experiments are reported in the figures and legends. Systat software was used for data analysis. Statistical significance between groups was determined by one-way ANOVA (analysis of variance) followed by Holm-Sidak test.

Figures

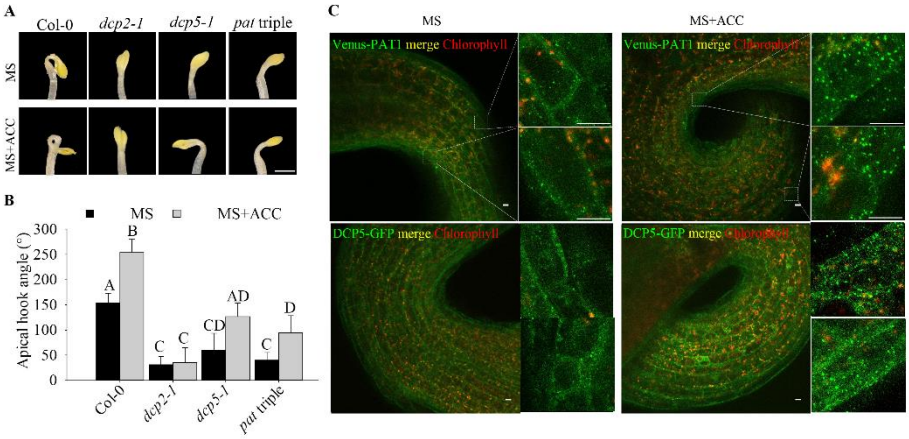

Fig 1. mRNA decapping deficiency causes deregulation of apical hooking. Hook phenotypes (**A**) and apical hook angles (**B**) in triple response to ACC treatment of etiolated Col-0, *dcp2-1*, *dcp5-1* and *pat* triple seedlings. The experiment was repeated 3 times, and representative pictures are shown. The scale bar indicates 1mm. (**C**) Representative confocal microscopy pictures of hook regions following ACC treatment. Dark-grown seedlings with either Venus-PAT1or DCP5-GFP on MS or MS+ACC plates for 4 days. Scale bars indicate 10 μm. Bars marked with the same letter are not significantly different from each other (P-value>0.05).

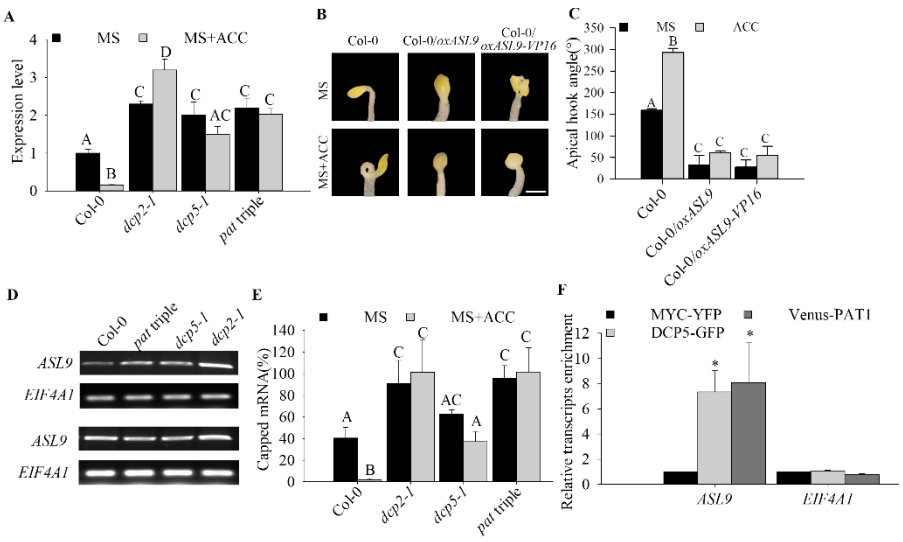

Fig 2. mRNA decay machinery targets *ASL9* for decay. (**A**) *ASL9* mRNA levels in cotyledons and hook regions of dark-grown Col-0, *dcp2-1*, *dcp5-1* and *pat* triple seedlings under control or ACC treatment. Error bars indicate SE (n = 3). Hook phenotypes(**B**) and apical hook angles(**C**) of triple response to ACC treatment of etiolated seedlings of Col-0, Col-0/*oxASL9* and Col-0/*oxASL9-VP16*. The experiment was repeated 3 times, and representative pictures are shown. The scale bar indicates 1mm. (**D**) Accumulation of capped transcripts of *ASL9* analyzed in 4-day-old MS grown etiolated seedlings of Col-0, *pat* triple, *dcp5-1* and *dcp2-1* by 5'-RACE-PCR. RACE-PCR products obtained using a low (upper panel) and high (bottom panel) number of cycles are shown. *EIF4A1* RACE-PCR products were used as loading control. (**E**) Capped *ASL9* transcript levels in cotyledons and hook regions of dark-grown Col-0, *dcp2-1*, *dcp5-1* and *pat* triple seedlings. Error bars indicate SE (n = 3). (**F**) Both DCP5 and PAT1 can bind *ASL9* transcripts. 4-day dark-grown plate seedlings with DCP5-GFP or Venus-PAT1were taken for the RIP assay. *ASL9* transcript levels were normalized to those in RIP of MYC-YFP as a non-binding control. *EIF4A1* was used as a negative control. Error bars indicate SE (n=3).

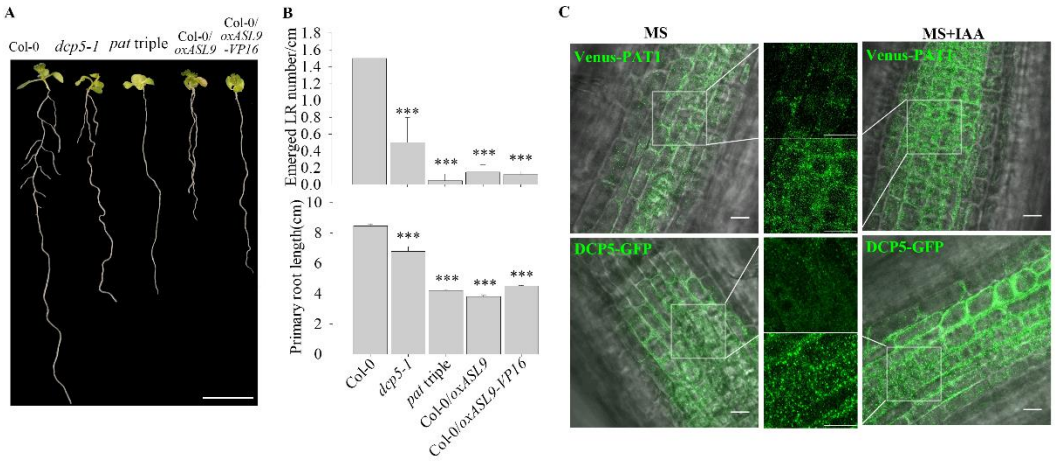

Fig 3. Accumulation of *ASL9* suppresses LR formation and primary root growth. Phenotypes (**A**), emerged LR density and primary root length (**B**) of 10-day old seedlings of Col-0, *dcp5-1*, *pat* triple, Col-0/*oxASL9* and Col-0/*oxASL9-VP16*. The experiment was repeated 4 times, and representative pictures are shown. The scale bar indicates 1cm. Bars marked with the same letter are not significantly different from each other (P-value>0.05). (**C**) Representative confocal microscopy pictures of root regions from 7-day old seedlings with either Venus-PAT1 or DCP5-GFP treated with MS or MS+0.2 µIAA for 15min. Scale bars indicate 10 µm.

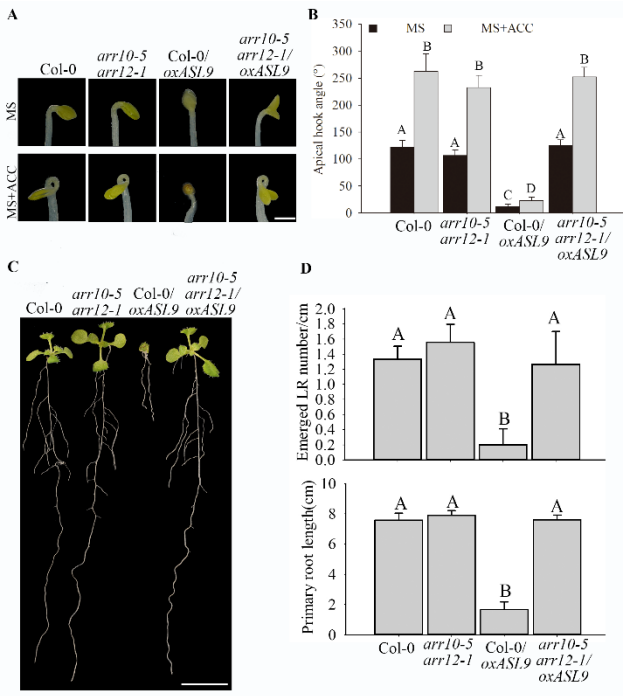

Fig 4. *ARR10* and *ARR12* loss-of-function restores apical hook, LR formation and primary root elongation in *ASL9* over-expressor. Hook phenotypes (**A**) and apical hook angles (**B**) in triple responses to ACC treatment of etiolated Col-0, *arr10-5arr12-1*, Col-0*/oxASL9* and *arr10-5arr12-1/oxASL9* seedlings. The treatment was repeated 3 times, and representative pictures are shown. The scale bar indicates 1mm. Phenotypes (**C**), emerged LR density and primary root length (**D**) of 10-day old seedlings of Col-0, *arr10-5arr12-1*, Col-0*/oxASL9* and *arr10-5arr12-1/oxASL9*. Treatment was repeated 3 times, and representative pictures are shown. The scale bar indicates 1cm. Bars marked with the same letter are not significantly different from each other (P-value>0.05).

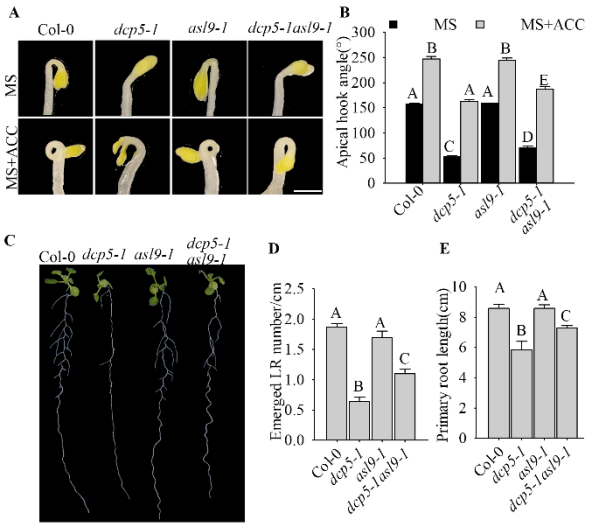

364 **Fig 5. *ASL9* directly contributes to apical hooking, LR formation and primary root elongation.**
365 Hook phenotypes (**A**) and apical hook angles (**B**) in triple responses to ACC treatment of etiolated Col-
366 0, *dcp5-1*, *asl9-1* and *dcp5-1asl9-1* seedlings. The treatment was repeated 3 times, and representative
367 pictures are shown. The scale bar indicates 1mm. Phenotypes (**C**), emerged LR density (**D**) and primary
368 root length (**E**) of 10-day old seedlings of Col-0, *dcp5-1*, *asl9-1* and *dcp5-1asl9-1*. Treatment was
369 repeated 3 times, and representative pictures are shown. The scale bar indicates 1cm. Bars marked with
370 the same letter are not significantly different from each other (P-value>0.05).

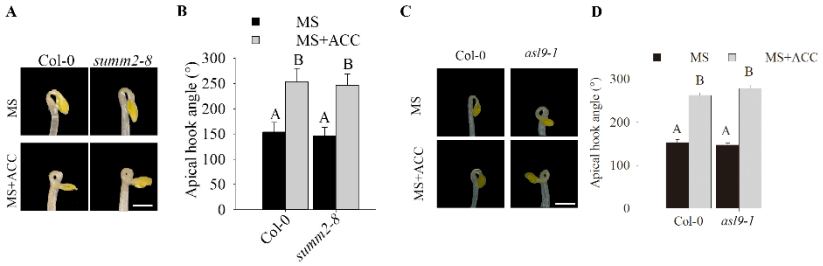

371 **Fig S1. Apical hook in *summ2-8* and *asl9-1* mutants.** Hook phenotypes (**A**) and apical hook angles (**B**)
372 in triple responses to ACC treatment of etiolated seedlings of Col-0 and *summ2-8*. Hook phenotypes (**C**)
373 and apical hook angles (**D**) in triple responses to ACC treatment of etiolated Col-0 and *asl9-1* seedlings.
374 The treatment was repeated 3 times, and representative pictures are shown. The scale bar indicates 1mm.

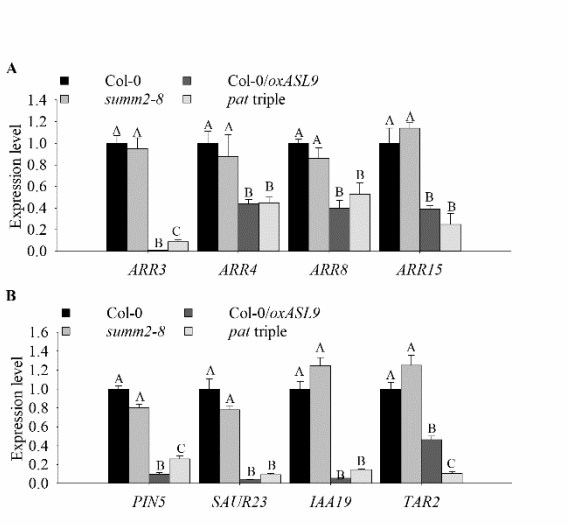

Fig S2. Cytokinin and auxin related genes expression in mRNA decay deficient mutant and *ASL9* over-expressor. Cytokinin pathway repressor genes(**A**) *ARR3*, *ARR4*, *ARR8* and *ARR15* and auxin pathway genes(**B**) *PIN5*, *SAUR23*, *IAA19 and TAR2* expression levels in 10-day-old seedlings of Col-0, *summ2-8*, Col-0/*oxASL9* and *pat1-1path1-4path2-1summ2-8.* The experiment was repeated 3 times, and representative pictures are shown. Bars marked with the same letter are not significantly different from each other (P-value>0.05).

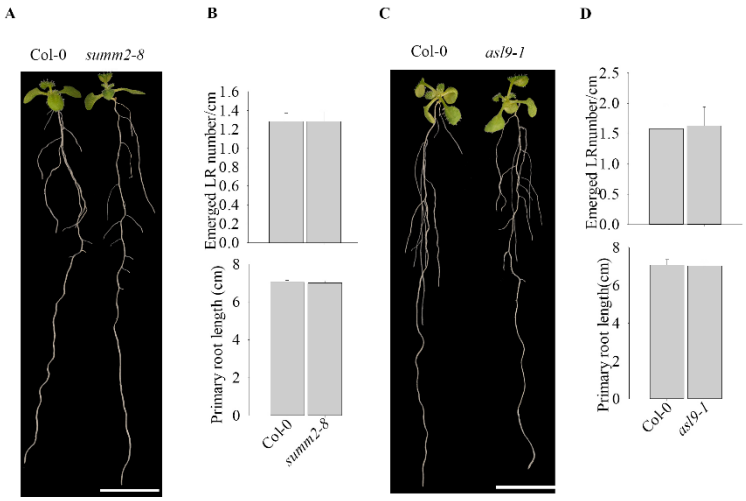

Fig S3. LR formation and primary root growth in *summ2-8* and *asl9-1* mutants. Phenotypes (**A**) emerged LR density and primary root length (**B**)of 10-day old seedlings of Col-0 and *summ2-8*. Phenotypes (**C**) emerged LR density and primary root length (**D**) of 10-day old seedlings of Col-0 and *asl9-1*. The scale bar indicates 1cm.

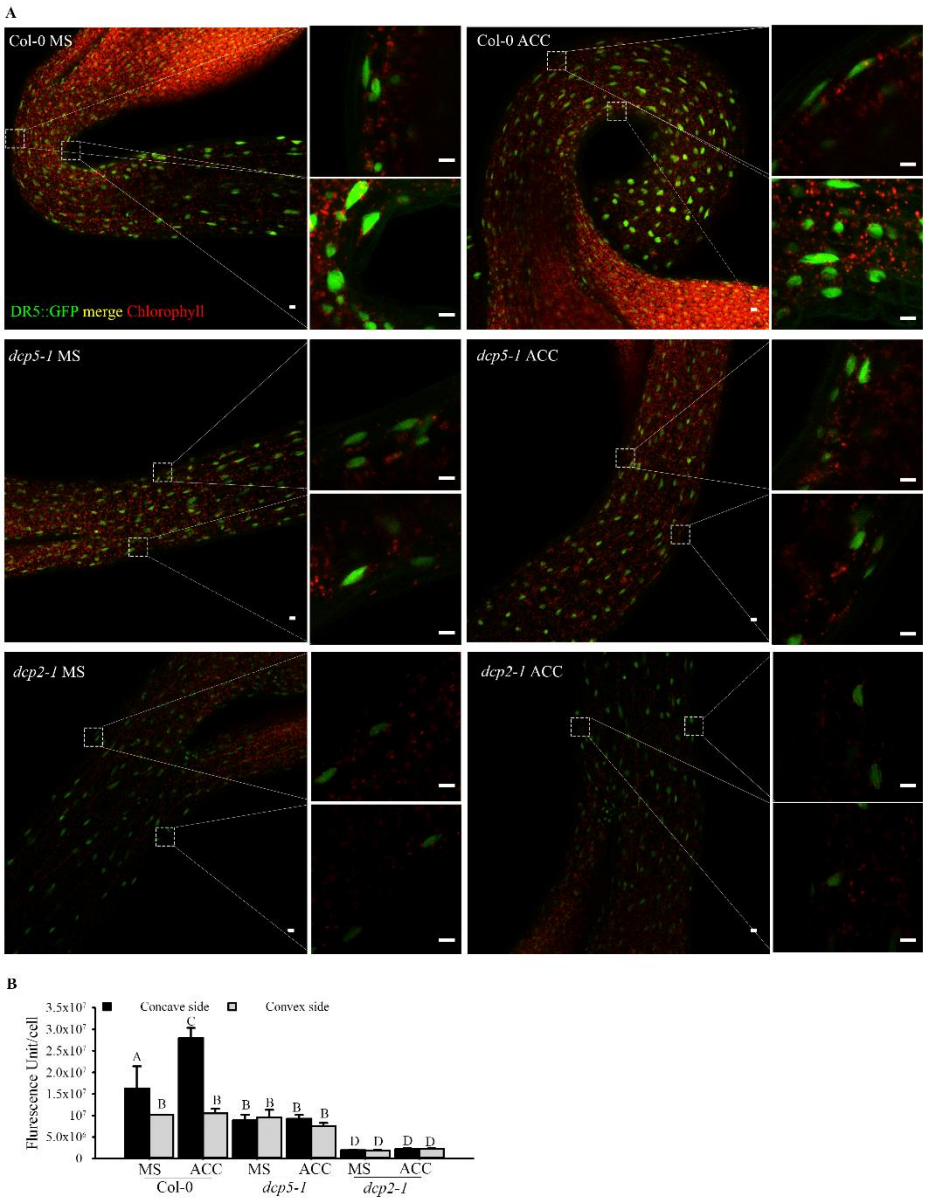

385 **Fig S4. Decapping mutants *dcp5-1* and *dcp2-1* exhibit repressed auxin responses in apical hook**
386 **regions.** Representative confocal microscopy pictures(**A**) and quantification(**B**) of GFP signals in
387 concave and convex side of apical hook regions of Col-0, *dcp5-1* and *dcp2-1* expressed with DR5::GFP
388 following ACC treatment. Seeds of Col-0/DR5::GFP, *dcp5-1*/DR5::GFP and *dcp2-1/* DR5::GFP on MS
389 or MS+ACC plates were vernalized 96hr and grown in dark for 4 days. Scale bars indicate 10μm. Bars
390 marked with the same letter are not significantly different from each other (P-value>0.05).

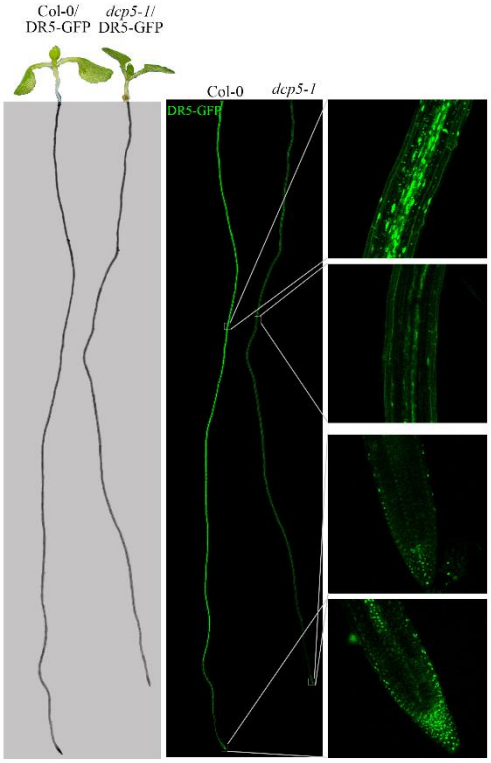

Fig S5. Decapping mutants *dcp5-1* exhibit repressed auxin responses in Root regions. Representative confocal microscopy pictures of GFP signals in root regions of 7-day old seedling of Col-0 and *dcp5-1* expressed with DR5::GFP. Seeds of Col-0/DR5::GFP and *dcp5-1*/DR5::GFP on MS plates were vernalized 96hr and grown vertically for 7 days. Scale bars indicate 10μm.

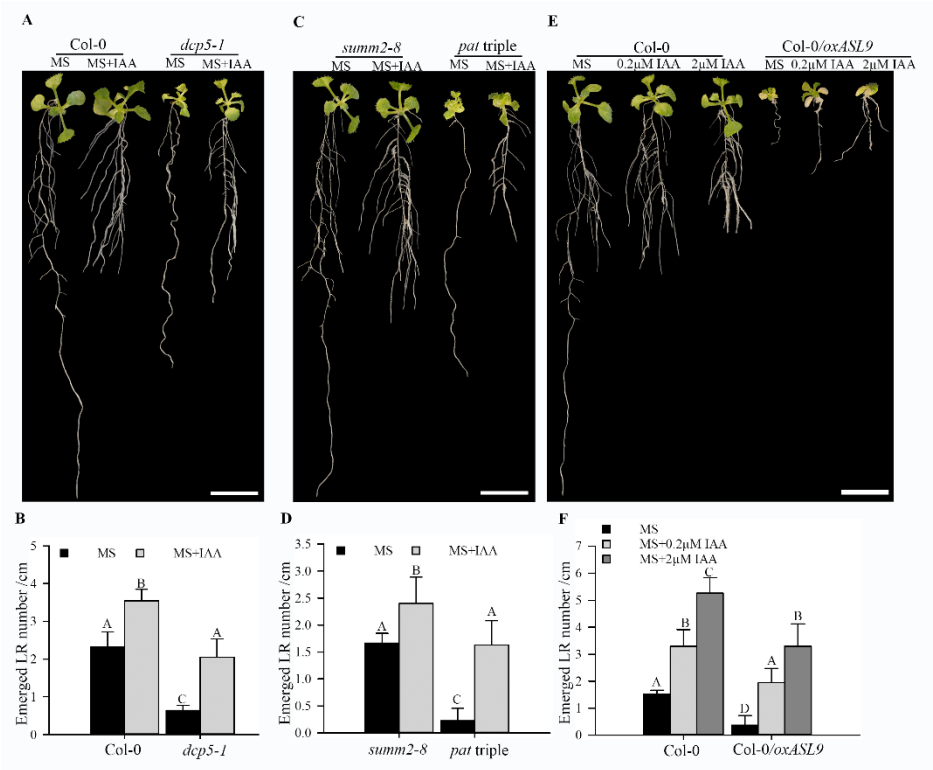

Fig S6. Auxin restores LR formation in mRNA decay deficient mutants and Col-0/*oxASL9*.

Phenotypes(**A**) and emerged LR density(**B**) of 14-day old seedlings of *summ2-8* and *pat1-1path1-4path2-1summ2-8* on MS or MS with 0.2μM IAA. Phenotypes (**C**) and emerged LR density (**D**) of 14-day old seedlings of Col-0 and *dcp5-1* on MS or MS with 0.2μM IAA. Phenotypes (**E**) and emerged LR density (**F**) of 14-day old seedlings of Col-0 and Col-0/*oxASL9* on MS, MS with 0.2μM IAA or MS with 2μM IAA. Seeds on MS plates were vernalized 96hrs and grown with 16/8 hrs light/dark at 21°C for 7 days. The seedlings were moved to MS or MS+IAA plates and grown vertically for 7 days. The treatment was repeated 3 times, and representative pictures are shown. The scale bar indicates 1cm. Bars marked the same letter are not significantly different from each other (P-value>0.05).

404 **Table S1. Mutants used in this study**

Mutant	Information	Source
path1-4	7bp deletion in Exon 2, frame shift and early stop codon	Zuo et al., 2022b
path2-1	35bp deletion in Exon 2, frame shift, early stop codon	Zuo et al., 2022b
asl9-1	SAIL_659_D08, T-DNA insertion in Exon 1	NASC (Nottingham, UK)
pat1-1	Salk_040660, T-DNA insertion in Exon 5	Roux et al., 2015
summ2-8	SAIL_1152A06, T-DNA insertion in Exon 1	Zhang et al., 2012
dcp5-1	Salk_008881, T-DNA insertion in 3'-UTR	Xu and Chua, 2009
dcp2-1	Salk_000519, T-DNA insertion in Exon 3	Xu et al., 2006
arr10-5	Salk_098604, T-DNA insertion in Exon 5	Ishida et al., 2008
arr12-1	Salk_054752, T-DNA insertion in Exon 3	Ishida et al., 2008

405

Table S2. Primers used in this study

Primer	Sequence	Use
genotyping		
LBb1.3	ATTTTGCCGATTTCGGAAC	Genotyping Salk lines
SAIL LB3	CATCTGAATTTCATAACCAATCTC	Genotyping Sail lines
SAIL_659_D08 LP	ATGTTGTACGTTGATTTGGGG	SAIL_659_D08 genotyping
SAIL_659_D08 RP	TATTCTTTACACGCGGTTTCG	SAIL_659_D08 genotyping
DCP2LP	TGATGGGGTTTTGTTTCAGTC	*dcp2* genotyping
DCP2RP	ACTATGATCAATGAGTGGCGG	*dcp2* genotyping
qPCR		
ASL9 for	CAAAAGGGTCACAGACACGGAA	qPCR of *ASL9*
ASL9 rev	GGCCTCGTACACCATCGAATC	qPCR of *ASL9*
EIF4A1F	GATCTGCACCAGAAGGCACA	qPCR of *EIF4A1*
EIF4A1R	CCCAGTACCAGACTGAGCCTGTTG	qPCR of *EIF4A1*
ARR3F	GAAACTCGCCGACGTGAAAC	qPCR of *ARR3*
ARR3R	TCCACAAGCGAAGTTGCAGA	qPCR of *ARR3*
ARR4F	ATGGCCAGAGACGGTGGTGTTTC	qPCR of *ARR4*
ARR4R	ATCTAATCCGGGACTCCTCATC	qPCR of *ARR4*
ARR8F	GACCCAAATGCACTCTCTACATC	qPCR of *ARR8*
ARR8R	CTCTTCAGCTCCTTCTTCCAAAC	qPCR of *ARR8*
ARR15F	GACGACTGTTGAGAGTGGGAC	qPCR of *ARR15*
ARR15R	CTCCTCTGCTCCTTCTATCATAC	qPCR of *ARR15*
PIN5-FW	CCATCGGCTCTATTGTCCTTG	qPCR of *PIN5*
PIN5-RV	GCGACGAGCACAGGTAGAGA	qPCR of *PIN5*
SAUR23 F	ATTCAAACTTTCAGACAAAAGAAATGG	qPCR of *SAUR23*
SAUR23 R	ACAAGGAAACAACTCTATCTCTAACT	qPCR of *SAUR23*
IAA19 F	GGTGACAACTGCGAATACGTTACCA	qPCR of *IAA19*
IAA19 R	CCCGGTAGCATCCGATCTTTTCA	qPCR of *IAA19*
TAR2 F	CATGATTTGGCTTACTATTGGCCACAG	qPCR of *TAR2*
TAR2 R	GTCTTTCACCAAAGCCCATCCAATC	qPCR of *TAR2*
ARR10F	GCTTCTGATGCTGGTTCCTT	qPCR of *ARR10*
ARR10R	CAATCACCTTCCGAGAAATCA	qPCR of *ARR10*
ARR12F	CTCCACGATGAAGCAGGAA	qPCR of *ARR12*
ARR12R	AACTAAACCCTCCATATCCCAAA	qPCR of *ARR12*
5'-RACE		
ASL9 inner	GGCCTCGTACACCATCGAATC	RACE inner PCR
ASL9 outer	ATGTCGATGTCACTGTAGAAG	RACE outer PCR
EIF4A1 inner	GGTTCTCTTGAAGACCCATGGCATC	RACE inner PCR
EIF4A1 outer	CCCAGTACCAGACTGAGCCTGTTG	RACE outer PCR

406

Acknowledgments

We thank Qi-Jun Chen for Phee401, Nam-Hai Chua for *dcp5-1* and *dcp2-1* seeds and Damien Garcia for DCP5-GFP marker line seeds. Special thanks to John Mundy for advice throughout the project and critically reading the manuscript. This work was supported by the Novo Nordisk Fonden and the Hartmanns Fond to MP (NNF18OC0052967 and A32638), the Institute Strategic Programme grant (BB/P013511/1) to the John Innes Centre and a PhD scholarship from China Scholarship Council to ZZ (201504910714).

ZZ, MER, and MP conceived and designed the experiments. ZZ, MER, JRC, YD, TY, SDH, EK, LØ and ER performed experiments. ZZ and MP analyzed the data. ZZ and MP wrote the manuscript.

The authors declare no competing interests.

Correspondence and requests for materials should be addressed to MP.

References

Balagopal, V., and Parker, R. (2009). Polysomes, P bodies and stress granules: states and fates of eukaryotic mRNAs. Curr Opin Cell Biol **21,** 403-408.

Bell, E.M., Lin, W.C., Husbands, A.Y., Yu, L.F., Jaganatha, V., Jablonska, B., Mangeon, A., Neff, M.M., Girke, T., and Springer, P.S. (2012). Arabidopsis LATERAL ORGAN BOUNDARIES negatively regulates brassinosteroid accumulation to limit growth in organ boundaries. P Natl Acad Sci USA **109,** 21146-21151.

Billou I, Xu J, Wildwater M, Willemsen V, Paponov I, Friml J, Heidstra R, Aida M, Palme K, and Scheres B. (2005). The PIN auxin efflux facilitator network controls growth and patterning in Arabidopsis roots. Nature **433**, 39–44.

Bleecker, A.B., Estelle, M.A., Somerville, C., and Kende, H. (1988). Insensitivity to Ethylene Conferred by a Dominant Mutation in *Arabidopsis thaliana*. Science **241,** 1086-1089.

Bonnerot C, Boeck R, Lapeyre B. (2000) The two proteins Pat1p (Mrt1p) and Spb8p interact in vivo, are required for mRNA decay, and are functionally linked to Pab1p. Mol Cell Biol **20:**5939–5946.

Brengues, M., Teixeira, D., and Parker, R. (2005). Movement of eukaryotic mRNAs between polysomes and cytoplasmic processing bodies. Science **310,** 486-489.

Brumos J, Robles LM, Yun J, Vu TC, Jackson S, Alonso JM, Stepanova AN. (2018). Local auxin biosynthesis is a key regulator of plant development. Developmental Cell **47**, 306–318.e5.

Charenton, C., Gaudon-Plesse, C., Fourati, Z., Taverniti, V., Back, R., Kolesnikova, O., Seraphin, B., and Graille, M. (2017). A unique surface on Pat1 C-terminal domain directly interacts with Dcp2 decapping enzyme and Xrn1 5 '-3 ' mRNA exonuclease in yeast. P Natl Acad Sci USA **114,** E9493-E9501.

Chaudhury, A.M., Letham, S., Craig, S., and Dennis, E.S. (1993). Amp1 - a Mutant with High Cytokinin Levels and Altered Embryonic Pattern, Faster Vegetative Growth, Constitutive Photomorphogenesis and Precocious Flowering. Plant J **4,** 907-916.

Chowdhury, A., Kalurupalle, S., and Tharun, S. (2014). Pat1 contributes to the RNA binding activity of the Lsm1-7-Pat1 complex. Rna-a Publication of the Rna Society **20,** 1465-1475.

Clough, S.J., and Bent, A.F. (1998). Floral dip: a simplified method for Agrobacterium-mediated transformation of Arabidopsis thaliana. Plant J **16,** 735-743.

Chicois, C., Scheer, H., Garcia, S., Zuber, H., Mutterer, J., Chicher, J., Hammann, P., Gagliardi, D., Garcia, D. (2018)The UPF1 interactome reveals interaction networks between RNA degradation and translation repression factors in Arabidopsis. Plant J. 96(**1**):119-132.

Coller, J., and Parker, R. (2005). General translational repression by activators of mRNA decapping. Cell **122,** 875-886.

Crisp, P.A., Ganguly, D., Eichten, S.R., Borevitz, J.O., and Pogson, B.J. (2016). Reconsidering plant memory: Intersections between stress recovery, RNA turnover, and epigenetics. Sci Adv **2**.

Crisp, P.A., Ganguly, D.R., Smith, A.B., Murray, K.D., Estavillo, G.M., Searle, I., Ford, E., Bogdanovic, O., Lister, R., Borevitz, J.O., Eichten, S.R., and Pogson, B.J. (2017). Rapid Recovery Gene Downregulation during Excess-Light Stress and Recovery in Arabidopsis. Plant Cell **29,** 1836-1863.

Dobin, A., Davis, C.A., Schlesinger, F., Drenkow, J., Zaleski, C., Jha, S., Batut, P., Chaisson, M., and Gingeras, T.R. (2013). STAR: ultrafast universal RNA-seq aligner. Bioinformatics **29,** 15-21.

Essig, K., Kronbeck, N., Guimaraes, J.C., Lohs, C., Schlundt, A., Hoffmann, A., Behrens, G., Brenner, S., Kowalska, J., Lopez-Rodriguez, C., Jemielity, J., Holtmann, H., Reiche, K., Hackermuller, J., Sattler, M., Zavolan, M., and Heissmeyer, V. (2018). Roquin targets mRNAs in a 3 '-UTR-specific manner by different modes of regulation. Nat Commun **9**.

Estelle, M.A., and Somerville, C. (1987). Auxin-Resistant Mutants of Arabidopsis-Thaliana with an Altered Morphology. Mol Gen Genet **206,** 200-206.

Fan, M.Z., Xu, C.Y., Xu, K., and Hu, Y.X. (2012). LATERAL ORGAN BOUNDARIES DOMAIN transcription factors direct callus formation in Arabidopsis regeneration. Cell Res **22,** 1169-1180.

Franks, T.M., and Lykke-Andersen, J. (2008). The Control of mRNA Decapping and P-Body Formation. Mol Cell **32,** 605-615.

Garneau, N.L., Wilusz, J., and Wilusz, C.J. (2007). The highways and byways of mRNA decay. Nat Rev Mol Cell Bio **8,** 113-126.

Geldner, N., Denervaud-Tendon, V., Hyman, D.L., Mayer, U., Stierhof, Y.D., and Chory, J. (2009). Rapid, combinatorial analysis of membrane compartments in intact plants with a multicolor marker set. Plant J **59,** 169-178.

Gerstberger, S., Hafner, M., and Tuschl, T. (2014). A census of human RNA-binding proteins. Nat Rev Genet **15,** 829-845.

Gloggnitzer, J., Akimcheva, S., Srinivasan, A., Kusenda, B., Riehs, N., Stampfl, H., Bautor, J., Dekrout, B., Jonak, C., Jimenez-Gomez, J.M., Parker, J.E., and Riha, K. (2014). Nonsense-Mediated mRNA Decay Modulates Immune Receptor Levels to Regulate Plant Antibacterial Defense. Cell Host Microbe **16,** 376-390.

Guzman, P., and Ecker, J.R. (1990). Exploiting the Triple Response of Arabidopsis to Identify Ethylene-Related Mutants. Plant Cell **2,** 513-523.

Hu, Y.M., Vandenbussche, F., and Van Der Straeten, D. (2017). Regulation of seedling growth by ethylene and the ethylene-auxin crosstalk. Planta **245,** 467-489.

Ishida, K., Yamashino, T., Yokoyama, A., and Mizuno, T. (2008). Three type-B response regulators, ARR1, ARR10 and ARR12, play essential but redundant roles in cytokinin signal transduction throughout the life cycle of Arabidopsis thaliana. Plant Cell Physiol **49,** 47-57.

Jang, G.J., Yang, J.Y., Hsieh, H.L., and Wu, S.H. (2019). Processing bodies control the selective translation for optimal development of Arabidopsis young seedlings. P Natl Acad Sci USA **116,** 6451-6456.

Jing, H.W., and Strader, L.C. (2019). Interplay of Auxin and Cytokinin in Lateral Root Development. Int J Mol Sci **20**.

Jung, J.K.H., and McCouch, S. (2013). Getting to the roots of it: genetic and hormonal control of root architecture. Front Plant Sci **4**.

Karimi, M., Depicker, A., and Hilson, P. (2007). Recombinational cloning with plant gateway vectors. Plant Physiol **145,** 1144-1154.

Kiss, D.L., Oman, K.M., Dougherty, J.A., Mukherjee, C., Bundschuh, R., and Schoenberg, D.R. (2016). Cap homeostasis is independent of poly(A) tail length. Nucleic Acids Res **44,** 304-314.

Laplaze, L., Benkova, E., Casimiro, I., Maes, L., Vanneste, S., Swarup, R., Weijers, D., Calvo, V., Parizot, B., Herrera-Rodriguez, M.B., Offringa, R., Graham, N., Doumas, P., Friml, J., Bogusz, D., Beeckman, T., and Bennett, M. (2007). Cytokinins act directly on lateral root founder cells to inhibit root initiation. Plant Cell **19,** 3889-3900.

Lehman, A., Black, R., and Ecker, J.R. (1996). HOOKLESS1, an ethylene response gene, is required for differential cell elongation in the Arabidopsis hypocotyl. Cell **85,** 183-194.

Li, X., Mo, X.R., Shou, H.X., and Wu, P. (2006). Cytokinin-mediated cell cycling arrest of pericycle founder cells in lateral root initiation of Arabidopsis. Plant Cell Physiol **47,** 1112-1123.

Liao, C.Y., Smet, W., Brunoud, G., Yoshida, S., Vernoux, T., and Weijers, D. (2015). Reporters for sensitive and quantitative measurement of auxin response (vol 12, pg 207, 2015). Nat Methods **12,** 1098-1098.

Lobel, J.H., Tibble, R.W., Gross, J.D. (2019). Pat1 activates late steps in mRNA decay by multiple mechanisms. P Natl Acad Sci USA **116 (47)**, 23512-23517

Malamy, J.E., and Benfey, P.N. (1997). Organization and cell differentiation in lateral roots of Arabidopsis thaliana. Development **124,** 33-44.

Matsumura, Y., Iwakawa, H., Machida, Y., and Machida, C. (2009). Characterization of genes in the ASYMMETRIC LEAVES2/LATERAL ORGAN BOUNDARIES (AS2/LOB) family in Arabidopsis thaliana, and functional and molecular comparisons between AS2 and other family members. Plant J **58,** 525-537.

Merret, R., Descombin, J., Juan, Y.T., Favory, J.J., Carpentier, M.C., Chaparro, C., Charng, Y.Y., Deragon, J.M., and Bousquet-Antonelli, C. (2013). XRN4 and LARP1 Are Required for a Heat-Triggered mRNA Decay Pathway Involved in Plant Acclimation and Survival during Thermal Stress. Cell Rep **5,** 1279-1293.

Miyamoto, T., Furusawa, C., and Kaneko, K. (2015). Pluripotency, Differentiation, and Reprogramming: A Gene Expression Dynamics Model with Epigenetic Feedback Regulation. Plos Comput Biol **11**.

Mylle, E., Codreanu, M.C., Boruc, J., and Russinova, E. (2013). Emission spectra profiling of fluorescent proteins in living plant cells. Plant Methods **9**.

Naito, T., Yamashino, T., Kiba, T., Koizumi, N., Kojima, M., Sakakibara, H., and Mizuno, T. (2007). A link between cytokinin and ASL9 (ASYMMETRIC LEAVES 2 LIKE 9) that belongs to the AS2/LOB (LATERAL ORGAN BOUNDARIES) family genes in Arabidopsis thaliana. Biosci Biotech Bioch **71,** 1269-1278.

Nakagawa, T., Kurose, T., Hino, T., Tanaka, K., Kawamukai, M., Niwa, Y., Toyooka, K., Matsuoka, K., Jinbo, T., and Kimura, T. (2007). Development of series of gateway binary vectors, pGWBs, for realizing efficient construction of fusion genes for plant transformation. J Biosci Bioeng **104,** 34-41.

Newman, R., Ahlfors, H., Saveliev, A., Galloway, A., Hodson, D.J., Williams, R., Besra, G.S., Cook, C.N., Cunningham, A.F., Bell, S.E., and Turner, M. (2017). Maintenance of the marginal-zone B cell compartment specifically requires the RNA-binding protein ZFP36L1. Nat Immunol **18,** 683-+.

Ozgur, S., Chekulaeva, M., and Stoecklin, G. (2010). Human Pat1b Connects Deadenylation with mRNA Decapping and Controls the Assembly of Processing Bodies. Mol Cell Biol **30,** 4308-4323.

Peer, W.A., Blakeslee, J.J., Yang, H.B., and Murphy, A.S. (2011). Seven Things We Think We Know about Auxin Transport. Mol Plant **4,** 487-504.

Perea-Resa, C., Hernandez-Verdeja, T., Lopez-Cobollo, R., Castellano, M.D., and Salinas, J. (2012). LSM Proteins Provide Accurate Splicing and Decay of Selected Transcripts to Ensure Normal Arabidopsis Development. Plant Cell **24,** 4930-4947.

Perea-Resa, C., Carrasco-Lopez, C., Catala, R., Tureckova, V., Novak, O., Zhang, W.P., Sieburth, L., Jimenez-Gomez, J.M., and Salinas, J. (2016). The LSM1-7 Complex Differentially Regulates Arabidopsis Tolerance to Abiotic Stress Conditions by Promoting Selective mRNA Decapping. Plant Cell **28,** 505-520.

Petersen, M., Brodersen, P., Naested, H., Andreasson, E., Lindhart, U., Johansen, B., Nielsen, H.B., Lacy, M., Austin, M.J., Parker, J.E., Sharma, S.B., Klessig, D.F., Martienssen, R., Mattsson, O., Jensen, A.B., and Mundy, J. (2000). Arabidopsis MAP kinase 4 negatively regulates systemic acquired resistance. Cell **103,** 1111-1120.

Riefler, M., Novak, O., Strnad, M., and Schmulling, T. (2006). Arabidopsis cytokinin receptor mutants reveal functions in shoot growth, leaf senescence, seed size, germination, root development, and cytokinin metabolism. Plant Cell **18,** 40-54.

Riehs-Kearnan, N., Gloggnitzer, J., Dekrout, B., Jonak, C., and Riha, K. (2012). Aberrant growth and lethality of Arabidopsis deficient in nonsense-mediated RNA decay factors is caused by autoimmune-like response. Nucleic Acids Res **40,** 5615-5624.

Rodriguez, E., Chevalier, J., Olsen, J., Ansbol, J., Kapousidou, V., Zuo, Z.L., Svenning, S., Loefke, C., Koemeda, S., Drozdowskyj, P.S., Jez, J., Durnberger, G., Kuenzl, F., Schutzbier, M., Mechtler, K., Ebstrup, E.N., Lolle, S., Dagdas, Y., and Petersen, M. (2020). Autophagy mediates temporary reprogramming and dedifferentiation in plant somatic cells. Embo J **39**.

Roux, M.E., Rasmussen, M.W., Palma, K., Lolle, S., Regue, A.M., Bethke, G., Glazebrook, J., Zhang, W.P., Sieburth, L., Larsen, M.R., Mundy, J., and Petersen, M. (2015). The mRNA decay factor PAT1 functions in a pathway including MAP kinase 4 and immune receptor SUMM2. Embo J **34,** 593-608.

Schaller, G.E., Bishopp, A., and Kieber, J.J. (2015). The Yin-Yang of Hormones: Cytokinin and Auxin Interactions in Plant Development. Plant Cell **27,** 44-63.

Smetana, O., Mäkilä, R., Lyu, M., Amiryousefi, A., Rodríguez, F. S., Wu, M., Solé-Gil, A., Gavarrón, M. L., Siligato, R., Miyashima, S., Roszak, P., Blomster,T., Reed, J.W., Broholm, A., and Mähönen, A. P. (2019). High levels of auxin signalling define the stem-cell organizer of the vascular cambium. Nature **565**, 485–489.

Smit, M. E., McGregor, S. R., Sun, H., Gough, C., Bågman, A.M., Soyars, C. L., Kroon, J. T., Gaudinier, A., Williams, C. J., Yang, X. (2020) A PXY-mediated transcriptional network integrates signaling mechanisms to control vascular development in Arabidopsis. Plant Cell, **32**, 319-335

Sorenson, R.S., Deshotel, M.J., Johnson, K., Adler, F.R., and Sieburth, L.E. (2018). Arabidopsis mRNA decay landscape arises from specialized RNA decay substrates, decapping- mediated feedback, and redundancy. P Natl Acad Sci USA **115,** E1485-E1494.

Streitner, C., Koster, T., Simpson, C.G., Shaw, P., Danisman, S., Brown, J.W.S., and Staiger, D. (2012). An hnRNP-like RNA-binding protein affects alternative splicing by in vivo interaction with transcripts in Arabidopsis thaliana. Nucleic Acids Res **40,** 11240-11255.

Su, Y.H., Liu, Y.B., and Zhang, X.S. (2011). Auxin-Cytokinin Interaction Regulates Meristem Development. Mol Plant **4,** 616-625.

Takahashi, K., and Yamanaka, S. (2006). Induction of pluripotent stem cells from mouse embryonic and adult fibroblast cultures by defined factors. Cell **126,** 663-676.

Tantikanjana, T., Yong, J.W.H., Letham, D.S., Griffith, M., Hussain, M., Ljung, K., Sandberg, G., and Sundaresan, V. (2001). Control of axillary bud initiation and shoot architecture in Arabidopsis through the SUPERSHOOT gene. Gene Dev **15,** 1577-1588.

Tatapudy, S., Aloisio, F., Barber, D., and Nystul, T. (2017). Cell fate decisions: emerging roles for metabolic signals and cell morphology. Embo Rep **18,** 2105-2118.

Vandenbussche F., Petrášek J., Žádníková P., Hoyerová K., Pešek B., Raz V., Swarup R., Bennett M., Zažímalová E., Benková E., and Van Der Straeten D. (2010) The auxin influx carriers AUX1 and LAX3 are involved in auxin-ethylene interactions during apical hook development in Arabidopsis thaliana seedlings. Development **137** (4): 597–606.

Weijers, D., Nemhauser, J., and Yang, Z.B. (2018). Auxin: small molecule, big impact. J Exp Bot **69,** 133-136.

Xiao, W., Molina, D., Wunderling, A., Ripper1, D., Vermeer, J.E.M., Ragni, L. (2020) Pluripotent pericycle cells trigger different growth outputs by integrating developmental cues into distinct regulatory modules. Current Biology **30**, 4384–4398

Xie, M.T., Chen, H.Y., Huang, L., O'Neil, R.C., Shokhirev, M.N., and Ecker, J.R. (2018). A B-ARR-mediated cytokinin transcriptional network directs hormone cross-regulation and shoot development. Nat Commun **9**.

Xu, C., Luo, F., and Hochholdinger, F. (2016). LOB Domain Proteins: Beyond Lateral Organ Boundaries. Trends Plant Sci **21,** 159-167.

Xu, J., and Chua, N.H. (2009). Arabidopsis Decapping 5 Is Required for mRNA Decapping, P-Body Formation, and Translational Repression during Postembryonic Development. Plant Cell **21,** 3270-3279.

Xu, J., and Chua, N.H. (2012). Dehydration stress activates Arabidopsis MPK6 to signal DCP1 phosphorylation. Embo J **31,** 1975-1984.

Xu, J., Yang, J.Y., Niu, Q.W., and Chua, N.H. (2006). Arabidopsis DCP2, DCP1, and VARICOSE form a decapping complex required for postembryonic development. Plant Cell **18,** 3386-3398.

Ye, L., Wang, X., Lyu, M., Siligato, R., Eswaran, G., Vainio, L., Blomster, T., Zhang, J., and Mähönen, A. P. (2021) Cytokinins initiate secondary growth in the Arabidopsis root through a set of LBD genes. Current Biology **31**, 3365-3373.

Yu, J.Y., Vodyanik, M.A., Smuga-Otto, K., Antosiewicz-Bourget, J., Frane, J.L., Tian, S., Nie, J., Jonsdottir, G.A., Ruotti, V., Stewart, R., Slukvin, I.I., and Thomson, J.A. (2007). Induced pluripotent stem cell lines derived from human somatic cells. Science **318,** 1917-1920.

Yu, X., Li, B., Jang, G.J., Jiang, S., Jiang, D.H., Jang, Y.Y., Wu, S.H., Shan, L.B., and He, P. (2019). Orchestration of Processing Body Dynamics and mRNA Decay in Arabidopsis Immunity. Cell Rep **28,** 2194-+.

Zhang, Z.B., Wu, Y.L., Gao, M.H., Zhang, J., Kong, Q., Liu, Y.A., Ba, H.P., Zhou, J.M., and Zhang, Y.L. (2012). Disruption of PAMP-Induced MAP Kinase Cascade by a Pseudomonas syringae Effector Activates Plant Immunity Mediated by the NB-LRR Protein SUMM2. Cell Host Microbe **11,** 253-263.

Zuo, Z., Roux, M.E., Sæmundsson, H.P., Müller, M., Munne Bosch, S., and Petersen, M. (2021). The *Arabidopsis thaliana* mRNA decay factor PAT1 functions in osmotic stress responses and decaps ABA-responsive genes. Febs Lett, **595**:253-263.

Zuo, Z., Roux, M.E., Rodriguez, E., and Petersen, M. (2022a). mRNA decapping factors LSM1 and PAT paralogs are involved in TuMV viral infection. Mol Plant Microbe Interact. 449 35(2): 125-130,

Zuo,Z., Roux,M.E., Dagdas, Y., Rodriguez, E., and Petersen, M. (2022b). PAT mRNA decapping factors function specifically and redundantly during development in Arabidopsis. BioRxiv 2022.07.06.498930; doi: https://doi.org/10.1101/2022.07.06.498930